Complex behavior in a simple system: low temperature Ag/Ag(100) growth revisited

Yunsic Shim and Jacques G. Amar
Department of Physics & Astronomy
University of Toledo, Toledo, Ohio 43606, USA
(Dated: June 2, 2009)

The experimentally observed non-monotonic temperature-dependence of the surface roughness in Ag/Ag(100) growth over the temperature range $T = 55-180$ K is examined. In general, we find that the surface roughness depends sensitively on a competition between a variety of low-barrier processes including downward funneling, edge-zipping and diffusion, atom-attraction, and interlayer diffusion at kinks. By taking these processes into account, along with the attraction of depositing atoms to microprotrusions, excellent agreement with experiment is obtained over the entire temperature range.

PACS numbers: 68.55.-a, 81.15.Aa, 81.15.-z

Recently, there has been a great deal of progress in understanding the morphological evolution in epitaxial thin film growth (for a recent review see Ref. 1), and a variety of effects and processes have been shown to play an important role. In addition to growth temperature, deposition flux, and deposition angle,[2] these include the effects of crystal geometry,[3] the Ehrlich-Schwoebel (ES) barrier to interlayer diffusion,[4] edge- and corner-diffusion,[5,6] and the attraction of depositing atoms to the substrate.[2,7] Understanding these effects is important, since they can have a strong effect on a variety of important film properties including the surface morphology.

One case of particular interest is that of Ag/Ag(100) growth for which an unusually complex dependence of the surface roughness on deposition temperature has been observed over the temperature range $T = 55$ K - 300 K.[8] In particular, as the temperature was reduced below 300 K, the roughness of 25 monolayer films was found to first increase - with a peak at approximately 220 K - and then decrease as the temperature was further reduced. As the temperature was decreased below 135 K, the roughness again increased - with a second low-temperature peak at approximately 90 K - and then decreased again as the temperature was further reduced to 55 K.

The non-monotonic behavior of the surface roughness at high temperature ($T = 135$ K - 300 K) has been explained by Stoldt et al.[8] In particular, the increase in the surface roughness as the temperature is decreased from 300 to 220 K is due to the increased effect of the ES barrier to interlayer diffusion as the temperature is decreased over this temperature range. Similarly, the decrease in the surface roughness as the temperature is further decreased from 220 K to 135 K has been explained by the increased role of downward funneling (DF)[9] of atoms deposited near step-edges, due to the increased island- and step-density as the monomer diffusion rate decreases. Using a simplified kinetic Monte Carlo (KMC) model which includes relatively small but non-zero barriers for DF of atoms deposited at non-fourfold hollow sites (e.g. 'restricted' DF), Stoldt et al[8] were able to partially explain the initial increase in roughness at low temperature ($T < 135$ K). However, the resulting model led to poor agreement with experiment and was also unable to explain the decrease in the roughness below 90 K. In addition, it leads to predictions[8,10] for the low-temperature thin-film vacancy density which are more than an order of magnitude higher than the results of recent parallel temperature-accelerated dynamics (par-TAD) simulations.[11]

Here we show that by taking into account the existence of very-low barriers for edge-smoothing ('edge-zipping') and DF at three-fold hollow sites, along with the effects of SR attraction of depositing atoms to microprotrusions, excellent quantitative agreement with experiment can be obtained over the temperature range $T = 55-110$ K. Furthermore, by taking into account the existence of low barriers for concerted interlayer diffusion at and near kinks, both qualitative and quantitative agreement with experiment can be obtained over the entire low-temperature range ($T = 55-135$ K) as well as at higher temperatures. We note that our model also leads to a negligible low-temperature vacancy density in good agreement with accelerated dynamics simulations of low-temperature Cu/Cu(100) growth.[11]

In order to include the effects of short-range (SR) attraction in our simulations, we have used a hybrid model which combines a one-atom molecular dynamics (MD) simulation of the deposition process with kinetic Monte Carlo (KMC) simulations of activated events. Following this method, the depositing atom is assumed to follow the trajectory determined by its interaction with the substrate (with the substrate atoms held fixed in their lattice positions) until its distance to the closest substrate atom is equal to the nearest-neighbor distance. The depositing atom is then placed at the nearest fcc lattice site, and unless this site is a four-fold hollow site or other site with a barrier for DF, assumed to undergo DF until it reaches a four-fold hollow site or "trap" site with a barrier for DF. We note that in recent simulations of normal incidence Cu/Cu(100) growth at $T = 160$ K,[14] the surface roughness obtained using this method was found to be only slightly lower than that obtained by carrying out a full MD simulation of the depositing atom and surrounding substrate. In order to check for the dependence on

interaction potential, our MD simulations were carried out using two different potentials: an embedded-atom method (EAM) potential[12] as well as a Lennard-Jones (LJ) Ag potential[13] with approximately the same cut-off as the EAM potential. However, since there was very little dependence on the potential, to save computation time most of our simulations were carried out using the simpler LJ Ag potential.

Fig. 1(a) shows the key low-barrier activated processes for DF included in our KMC simulations which become active over the temperature range $55 - 110$ K. As in Ref. 8, we assume that DF is effectively instantaneous for atoms deposited at non-fourfold-hollow sites with coordination number $m < 3$ (where m is the number of nearest-neighbors for a given atom) as well as for atoms with $m = 3$ on (111) microfacets, since the barriers for these transitions are less than 0.1 eV. Based on similar observations, we also assume instantaneous DF for atoms with only 2 support sites, regardless of the number of in-plane bonds. In agreement with Ref. 8, we also assume that for atoms at 3-fold support sites with 2 in-plane lateral bonds ("3+2"), the barrier for DF is 0.25 eV, while the barrier for atoms with 3-fold support sites with 3 in-plane lateral bonds is somewhat larger (0.30 eV). However, in contrast to Ref. 8, in which DF barriers of 0.15 eV (0.25 eV) were assumed for atoms at sites with three supporting atoms and 0 (1) lateral bond respectively, here we assume that DF is essentially instantaneous for such sites, since our EAM calculations yield values less than 0.1 eV.

Also shown in Fig. 1 are the barriers for a variety of intralayer activated processes, since in contrast to Ref. 8 we do not assume instantaneous island restructuring to form square islands. Except for the processes of edge-diffusion and 'atom-attraction' shown in Figs. 1(c)(i) and 1(c)(ii), all barriers for intralayer diffusion were calculated based on the results of EAM calculations by Furman et al[16] in which the activation energies were calculated as a function of the occupation numbers of the 7 sites surrounding the moving atom labelled 1 through 7 in Fig. 1(b)(0). However, since the effect of sites 6 and 7 on the activation barrier is relatively weak, for simplicity in our KMC model we have only used the occupation numbers of sites $1 - 5$, and have assumed that sites 6 and 7 are empty. In particular, as shown in Fig. 1(b), there exists a very low barrier of 0.16 eV for an atom to be "attracted" to an empty site with two lateral bonds ('edge-zipping'). Such 'edge-zipping' processes tend to enhance the regularity of step-edges thus suppressing DF. In addition to these EAM-based barriers, we have also included, based on density-functional-theory calculations,[17] a barrier of 0.30 eV for the diffusion of singly-bonded atoms along island-edges ("edge diffusion") as shown in Fig. 1(c)(i). We note that this barrier is significantly lower than the barrier[17] (0.45 eV) for monomer diffusion on a flat terrace. Since the activation energy for the related process of "atom-attraction" shown in Fig. 1(c)(ii) is expected to be close to the edge-diffusion barrier, a comparable value

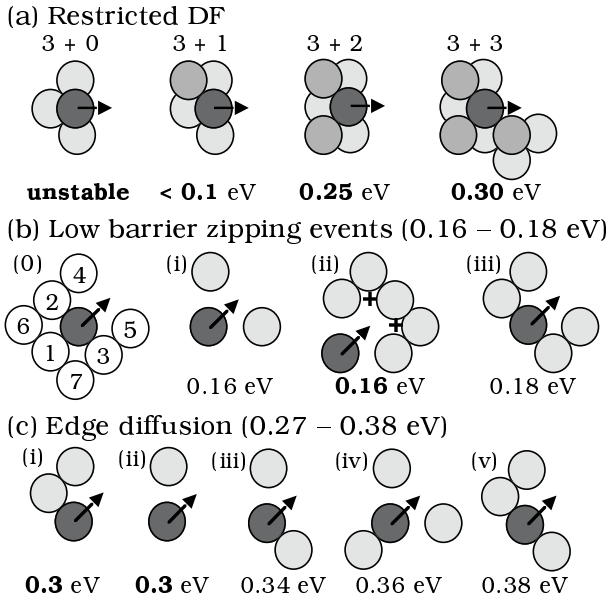

FIG. 1: Key low-barrier activated processes (boldface) for DF and intralayer diffusion: (a) DF for atoms at 3-fold hollow sites (b) low-barrier edge-zipping (c) higher barrier processes including (i) edge-diffusion and (ii) atom-attraction. Also shown in (c) iii-v are some representative higher barrier processes. Sites labeled "+" in (b)(ii) indicate 3-fold hollow sites which are converted to 4-fold hollow sites by edge-zipping.

of 0.3 eV has also been assumed for this process.

In addition to the processes shown in Fig. 1, our model includes a variety of other intralayer diffusion processes with higher activation barriers,[16] as well as a high barrier[8] (0.51 eV) for monomer descent at close-packed step-edges. However, since the barriers for these moves are all greater than 0.45 eV, they are only relevant above 165 K. Thus, in addition to the SR attraction of depositing atoms to the substrate, our model includes the following processes: (i) DF for atoms with $m \leq 3$ as well as for atoms at $3 + 1$ sites and all two-fold hollow sites (ii) restricted DF with an activation barrier of 0.25 eV (0.30 eV) for atoms at three-fold hollow sites with 2 (3) in-plane bonds (iii) low barrier and very low barrier edge-smoothing moves. For all activated events a prefactor of 10^{12} s^{-1} is assumed.[16] In order to compare with the experiment of Ref. 8, our simulations were carried out using the experimental deposition rate of 0.02 ML/s.

Using this model, the experimentally observed non-monotonic behavior of the surface roughness over the temperature range $55 - 110$ K may be explained as follows. As the temperature is decreased from 110 K to 85 K the DF of atoms deposited at "3+3" sites (with activation energy of 0.3 eV) is first suppressed at 110 K, followed by the suppression of DF at "3+2" sites at 90 K, thus leading to an increase in the surface roughness. However, as the temperature is further reduced below 85 K, the very-low-barrier edge-zipping mechanism - which can convert 3-fold hollow sites to stable 4-fold hollow

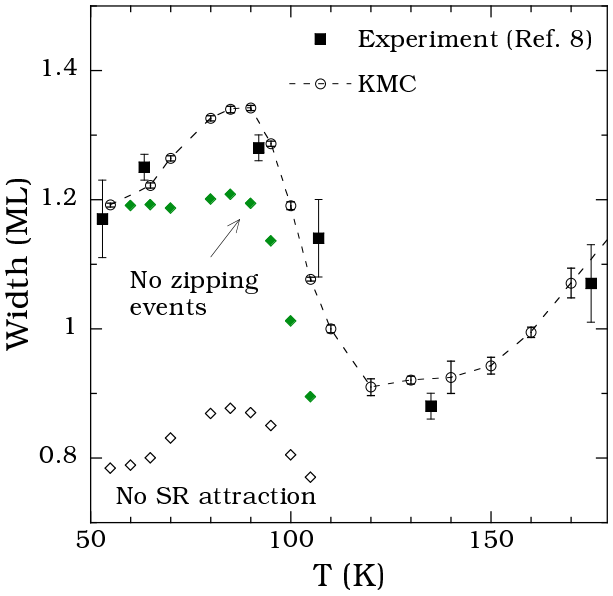

FIG. 2: Comparison between simulations and experimental results (filled squares) for surface roughness at thickness of 25 ML as function of deposition temperature.

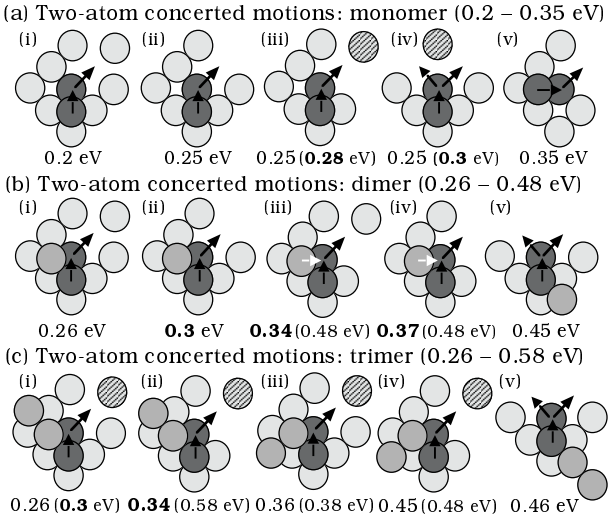

FIG. 3: Low-barrier interlayer diffusion processes for (a) monomers (b) dimers and (c) trimers near kinks which become active above 110 K. Activation barriers in boldface correspond to dominant processes observed in KMC simulations. Barriers in parentheses in (b) correspond to motion of "upper atom" (white arrow) "away from kink". Barriers in parentheses in (c) correspond to configurations without cross-hatched atom.

sites, as shown in Fig. 1(b)(ii) - is also suppressed. This leads to an increase in the amount of DF thus leading to a decrease in the surface roughness.

Fig. 2 shows our simulation results for the surface roughness along with the corresponding experimental results of Stoldt et al.[8] As can be seen, there is excellent quantitative agreement with experiment for $T = 55-110$ K. In contrast, if we remove the low-barrier zipping events shown in Fig. 1(b), then the surface roughness increases approximately monotonically with decreasing temperature over this temperature range. We note that this behavior is very similar to that found in Ref. 8 using a model which does not take into account the effects of SR attraction or the existence of finite barriers for edge-smoothing. This indicates that the inclusion of low-barrier zipping events is crucial to explain the experimentally observed non-monotonic behavior. Also shown in Fig. 2 are results obtained in the absence of SR attraction. While the experimentally observed non-monotonic behavior is still reproduced in this case, the surface roughness is significantly lower than in experiment, thus indicating that the attraction of depositing atoms to microprotrusions also plays a crucial role in determining the surface roughness.

We now consider the temperature range from 110 K to 135 K. We note that over this temperature range both edge-diffusion and atom-attraction become active, even though terrace diffusion of isolated monomers and interlayer diffusion at close-packed step-edges remain inactive. In particular, due to the increased effects of edge-diffusion, which tends to regularize step-edges and thus reduce DF, one expects the surface roughness to increase with increasing temperature over this temperature range. This is in contrast to the experimental results of Ref. 8 which indicate a further decrease in the roughness. However, by including in our simulations the low-barrier concerted interlayer diffusion processes for monomers, dimers, and trimers near kinks shown in Fig. 3 - which also become active over this temperature range - good agreement with experiment is obtained as shown in Fig. 2. Interestingly, the origin of the low activation barriers shown in Fig. 3 is the same as for edge-diffusion and edge-zipping, e.g. the existence of "side-atoms" which can attract the displaced atoms as they move to their new sites. Accordingly, as shown in Fig. 3, the interlayer diffusion barrier is even lower when there are two "attracting" side-atoms corresponding to a "double-kink" rather than one.

We note that the interlayer diffusion barriers shown in Fig. 3 were calculated either directly using the Voter-Chen EAM potential for Ag,[12] or by carrying out par-TAD annealing simulations of representative configurations, while a prefactor of 10^{13} s^{-1} was assumed for all interlayer diffusion moves.[18] We also note that while the 0.3 eV monomer interlayer diffusion process shown in Fig. 3(a)(iv) - for which the activation barrier has been previously calculated in Ref. 15 - plays an important role, the even lower barrier process shown in Fig. 3(a)(iii) is also important. Due to the high dimer and trimer density over this temperature range, the low-barrier "dimer" and "trimer" interlayer diffusion processes shown in Figs. 3(b)(ii)-(iv) and 3(c)(ii) also play important roles. For comparison, also shown in Fig. 3 are a number of other interlayer diffusion processes with significantly higher bar-

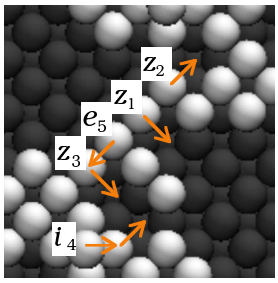

FIG. 4: Sequence of zipping (z), interlayer diffusion (i) and edge-diffusion (e) moves observed in 5 msec parTAD annealing simulation of representative configuration at 120 K.

riers.

Finally, we consider the surface roughness for $T > 135$ K. As can be seen in Fig. 2, due primarily to the increased effects of edge-diffusion and edge-zipping, which suppress interlayer diffusion by decreasing the kink density, but also due to "atom-attraction" (which tends to suppress interlayer diffusion at kinks by forming dimers and trimers) the surface roughness increases with increasing temperature in good agreement with experiment. Thus, our results indicate that over the temperature range from 110 to 180 K, the surface roughness depends sensitively on a competition between a variety of low-barrier processes including interlayer diffusion at kinks, edge-diffusion, edge-zipping, and atom-attraction.

Interestingly, while the overall effect of edge-zipping is to enhance the surface roughness by regularizing step-edges and suppressing DF, for $T > 110$ K it can also promote interlayer diffusion. As an illustration of how edge-zipping can enhance interlayer diffusion over this temperature range, Fig. 4 shows a sequence of configurations obtained in larger-scale parTAD simulations at 120 K. As can be seen, a sequence of zipping moves occurs before the atom in the upper layer can exchange at a kink site via the low-barrier (0.2 eV) process shown in Fig. 3(a)(i).

In conclusion, we have shown that by taking into account the existence of low-barrier processes for step-edge smoothing, DF, and interlayer diffusion, as well as the SR attraction of depositing atoms to microprotrusions, the dependence of the surface roughness in Ag/Ag(100) growth over the temperature range $55 - 180$ K can be quantitatively explained. In particular, while the increase in the roughness as the temperature is decreased from 110 K to 90 K is due to the suppression of DF of atoms deposited at "3+2" and "3+3" sites, the decrease in the roughness as the temperature is reduced below 90 K is due to the suppression of edge-zipping along with the existence of low-barrier processes for DF. In contrast, the decrease in the surface roughness from 110 K to 135 K is primarily due to the presence of low-barrier processes for interlayer diffusion at kinks which "turn-on" over this temperature range. Finally, for $T > 135$ K the increased effects of edge-diffusion lead to a decreased kink density which suppresses the low-barrier mechanisms for interlayer diffusion resulting in an increase in the roughness with increasing temperature. It is the complex interplay between all of these different processes which leads to the non-monotonic temperature-dependence observed in experiment.

Acknowledgments

This work was supported by NSF grant DMR-0606307 as well as by a grant of computer time from the Ohio Supercomputer Center.

[1] J.W. Evans, P.A. Thiel, and M.C. Bartelt, Surf. Sci. Rep. **61**, 1 (2006).
[2] S. van Dijken, L.C. Jorritsma, and B. Poelsema, Phys. Rev. Lett. **82**, 4038 (1999).
[3] M. C. Bartelt and J. W. Evans, Phys. Rev. Lett. **75**, 4250 (1995).
[4] G. Ehrlich and F. Hudda, J. Chem. Phys. **44**, 1039 (1966); R.L. Schwoebel, J. Appl. Phys. **40**, 614 (1969).
[5] M.V. Ramana Murty and B. H. Cooper, Phys. Rev. Lett. **83**, 352 (1999).
[6] O. Pierre-Louis, M. R. D'Orsogna, and T. L. Einstein, Phys. Rev. Lett. **82**, 3661 (1999).
[7] F. Montalenti and A.F. Voter, Phys. Rev. B **64**, 081401(R) (2001); J. Yu and J.G. Amar, Phys. Rev. Lett. **89**, 286103 (2002).
[8] C. R. Stoldt, K.J. Caspersen, M.C. Bartelt, C.J. Jenks, J.W. Evans, and P.A. Thiel, Phys. Rev. Lett. **85**, 800 (2000).
[9] J. W. Evans, D. E. Sanders, P. A. Thiel, and A. E. DePristo, Phys. Rev. B **41**, R5410 (1990).
[10] K.J. Caspersen and J.W. Evans, Phys. Rev. B **64**, 075401 (2001).
[11] Y. Shim, V. Borovikov, B.P. Uberuaga, A.F. Voter, and J.G. Amar, Phys. Rev. Lett. **101**, 116101 (2008).
[12] A. F. Voter, in *Intermetallic Compounds: Principles and Practice*, edited by J.H. Westbrook and R.L. Fleischer (Wiley and Sons, Ltd, New York, 1995), Vol. 1, p. 77.
[13] P. Cuan, D. R. Mckenzie and B. A. Pailthope, J. Phys.: Condens. Matter **8**, 8753 (1996).
[14] V. Borovikov, Y. Shim, and J.G. Amar, Phys. Rev. B **76**, 241401(R) (2007).
[15] U. Kurpick and T.S. Rahman, Phys. Rev. B **57**, 2482 (1998).
[16] I. Furman, O. Biham, J.-K. Zuo, A.K. Swan, and J.F. Wendelken, Phys. Rev. B **62**, R10649 (2000).
[17] B. D. Yu and M. Scheffler, Phys. Rev. Lett. **77**, 1095 (1996).
[18] For some of the configurations shown in Fig. 3, a range of activation energies was obtained in our parTAD simulations, due to differences in the representative configurations at longer ranges. In this case, an average value was used for the activation barrier.